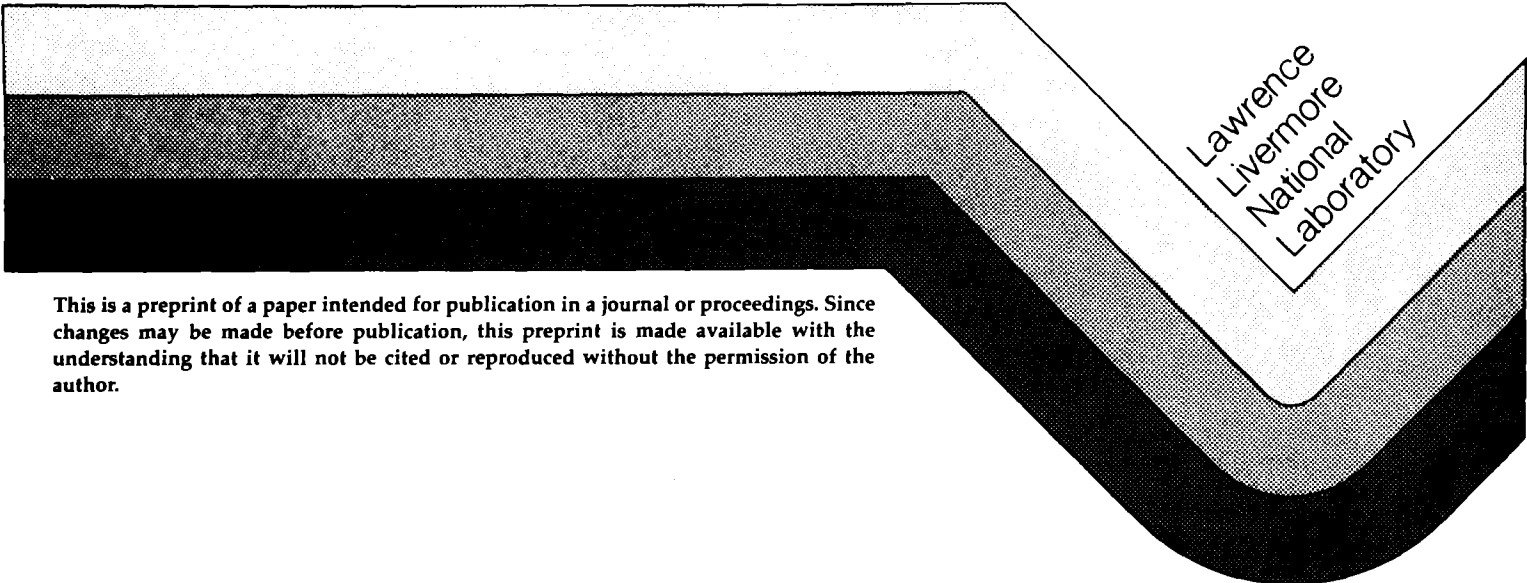


MIRROR THEORY APPLIED TO TOROIDAL SYSTEMS

Ronald H. Cohen

This paper was prepared for submittal to  
International School of Plasma Physics  
Varenna, Italy  
September 1-11, 1987

August 25, 1987



Lawrence  
Livermore  
National  
Laboratory

This is a preprint of a paper intended for publication in a journal or proceedings. Since changes may be made before publication, this preprint is made available with the understanding that it will not be cited or reproduced without the permission of the author.

#### DISCLAIMER

This document was prepared as an account of work sponsored by an agency of the United States Government. Neither the United States Government nor the University of California nor any of their employees, makes any warranty, express or implied, or assumes any legal liability or responsibility for the accuracy, completeness, or usefulness of any information, apparatus, product, or process disclosed, or represents that its use would not infringe privately owned rights. Reference herein to any specific commercial products, process, or service by trade name, trademark, manufacturer, or otherwise, does not necessarily constitute or imply its endorsement, recommendation, or favoring by the United States Government or the University of California. The views and opinions of authors expressed herein do not necessarily state or reflect those of the United States Government or the University of California, and shall not be used for advertising or product endorsement purposes.

# MIRROR THEORY APPLIED TO TOROIDAL SYSTEMS

*Ronald H. Cohen*

Lawrence Livermore National Laboratory  
University of California  
Livermore, California, 94550 USA

## ABSTRACT

Central features of a mirror plasma are strong departures from Maxwellian distribution functions, ambipolar potentials and densities which vary along a field line, end losses, and the mirror field itself. To examine these features, mirror theorists have developed analytical and numerical techniques to solve the Fokker-Planck equation, evaluate the potentials consistent with the resulting distribution functions, and assess the microstability of these distributions. Various combinations of mirror-plasma features are present and important in toroidal plasmas as well, particularly in the edge region and in plasmas with strong r.f. heating. In this paper we survey problems in toroidal plasmas where mirror theory and computational techniques are applicable, and discuss in more detail three specific examples: calculation of the toroidal generalization of the Spitzer-Härm distribution function (from which trapped-particle effects on current drive can be calculated), evaluation of the nonuniform potential and density set up by pulsed electron-cyclotron heating, and calculation of steady-state distribution functions in the presence of strong r.f. heating and collisions.

## **I. Introduction**

The international magnetic fusion research effort is becoming ever more heavily concentrated on toroidal devices. While many of the theoretical issues relevant to these devices are specifically connected to the toroidal configuration, there are also aspects of toroidal devices which are distinctly mirror-like, presenting opportunities for mirror theorists to apply their expertise. The purpose of this paper is to survey these areas and to describe in some detail three specific examples of toroidal-theory problems whose solution benefited from mirror-theory input.

The paper is organized as follows. In Section II we list some intrinsic features of mirror plasmas and indicate where they occur in toroidal devices. The next three sections are devoted to the specific examples: Section III describes a calculation of trapped-particle effects on current drive; Section IV discusses electron-cyclotron-heating (ECRH)-driven potentials; Section V discusses the calculation of distribution functions strongly heated by waves. Section VI is our survey of other areas where mirror theory has potential impact. Concluding remarks are given in Section VII.

## **II. Intrinsic Features of Mirror Plasmas**

Mirror plasmas have a number of features which are intrinsic to the configuration. These include the mirror field itself, endloss, strongly non-Maxwellian distribution functions, and potential and density variations along a field line. In this section, for each of these features, we briefly review the origin and consequences for mirror machines, mention some relevant theoretical tools, and indicate where the same or closely related features occur in toroidal devices.

The most obvious feature of a mirror machine is the mirror property itself, which results in the division of electron and ion phase space into regions of trapped particles which reflect off of the magnetic gradient, and passing particles which are lost from the system. Tandem-mirror and multiple-mirror machines are additionally complicated by the presence of particles trapped in different cells and particles which pass between different cells but do not reach the ends of the system. Mirror theory must thus contend with the resulting partition of a species into distinct groups with different confinement properties and different axial extents, and, for each group, axial variations of densities, collisionalities, etc. For many mirror-theory problems, one can eliminate spatial dependence by exploiting the largeness of the bounce frequency to construct bounce-averaged equations. The residual effects of the mirror field are that the resulting energy-magnetic-moment space is divided into passing and trapped regions and, in the case of multiple-well mirrors, is multiply sheeted, and that the coefficients in the kinetic equations are averages. Tokamaks, stellerators and bumpy toruses all have mirror fields; bean-shaped tokamaks and stellerators have coupled non-identical mirrors, like a tandem mirror.

Studies of phenomena associated with trapped particles in these devices are essentially mirror-physics studies, and tools originally employed for mirror studies, such as bounce-averaged Fokker-Planck codes (see, *e.g.*, Ref. 1), and analytic approximations like the square-well approximation for the collision operator, are now being applied to these devices [2,3]. Bean-shaped tokamaks have a particularly striking resemblance to tandem mirrors, as will be discussed in Sec. VI.

The open-ended property of the mirror field leads to direct losses to the end walls. In the bounce-averaged limit, particles which pass over the highest mirror (more precisely, the highest combined electrostatic and magnetic hill) in the system are lost; the distribution function for these particles must vanish. Consequences include non-Maxwellian distributions, axial potential and density variations, and a fundamental limit on the confinement of trapped particles due to collisional detrapping. The latter consequence has been the subject of much theoretical work [4-8]. In a tokamak, endlosses occur on edge-plasma field lines which strike a wall, a divertor or a limiter. It has been suggested [9, 10] that this endloss is related to the observation of the H mode. A closely related phenomenon which can occur further away from the edge of a toroidal device is rapid loss (faster than collisional replenishment) due to bad drifts. This has been discussed in connection with trapped alpha particles [11] and particles trapped in a toroidal well in a stellerator or a rippled tokamak [12], and has been proposed as a major limitation on the operation of the bumpy torus EBT-S [13].

Another inherent feature of mirror machines is strongly non-Maxwellian distribution functions. In the bounce-average limit, non-Maxwellian distributions are inevitable because of the vanishing of the distribution function in the loss region. While it is possible to create electrostatic potentials which confine some species, shifting the velocity-space loss region out to a high-energy tail of an otherwise Maxwellian distribution, the loss region must extend into the bulk for at least one species. Often there is a deliberate attempt to enhance the departure of distribution functions from Maxwellian, through strong radio-frequency (r.f.) heating or neutral-beam injection, to weigh more heavily a good-curvature region (as in the anchor of a tandem mirror), or to manipulate the electrostatic potential. Thus mirror experimentalists became the experts at producing, and theorists at calculating, strongly non-Maxwellian distributions. As these distributions typically contained ample drive for microinstability, mirror machines have for many years provided fertile ground for calculation of loss-cone and anisotropy-driven instabilities, and for the invention of schemes to manipulate the distributions so as to minimize these instabilities [14,15]. Tokamaks, too, have significantly non-Maxwellian distributions, some of which, like those associated with runaway electrons in the ohmic field, have been studied for many years. More recently, tokamak physicists have been considering non-Maxwellian distributions closer to the mirror variety:

distribution functions which vanish in some region due to direct particle losses, as discussed in the preceding paragraph, and distribution functions which are appreciably distorted from Maxwellian by strong r.f. heating in order to enhance current drive or improve stability.

Because of the difference in electron and ion collisionalities, mirror machines invariably develop electrostatic potential variations along field lines. This tendency was exploited in the tandem mirror, and enhanced by r.f. heating in the thermal-barrier tandem mirror. The potentials can be beneficial for axial confinement, but were shown to be a source of enhanced radial transport [16,17]. In tokamaks, neutral beam injection [18] and electron- or ion-cyclotron resonance heating [19,20] can again produce potential variations along field lines; this is the subject of Sec. IV.

### III. Trapped-Particle Effects on Current Drive

This section is the first of three which present examples of tokamak-theory problems whose solutions were facilitated by mirror-theory ideas. In this section we discuss trapped-particle effects on radio-frequency-driven currents. The calculation is discussed in greater detail in Ref. 3. The particular process nominally under consideration is electron-cyclotron resonance heating (ECRH), but the calculation applies equally well to lower-hybrid and even neutral-beam heating, so long as the current carriers are at energies significantly greater than thermal.

Trapped particles degrade current-drive efficiency because they absorb energy without producing current, and because a wave-induced push of an initially passing particle into the trapped-particle part of phase space leads to an increment of current opposite to that produced when the pushed particle remains passing. To calculate the current, we follow Antonsen, Chu and Hui [21], who demonstrated that the wave-induced current for any wave could be expressed in terms of the solution to an adjoint problem, which is a generalization of the Spitzer-Härm problem. The wave-induced current density is given by:

$$\frac{J_{\parallel}}{B} = \left\langle \int d^3p \Gamma_w \cdot \frac{\partial}{\partial \mathbf{p}} G \right\rangle \quad (1)$$

where  $\langle \rangle$  denotes a flux-surface average (or equivalently, a  $ds/B$  average, where  $s$  is arc length along a field line) and  $G = e \langle B_t/R \rangle^{-1} \exp(\varepsilon/T)g$ . Here  $R^{-1} \equiv |\nabla \phi|$ ,  $\phi$  is the toroidal angle,  $\varepsilon$  is the electron energy,  $T$  is the temperature of the background electrons used to construct the linearized collision operator,  $B_t$  is the toroidal magnetic field, and  $g$  is the Spitzer-Härm distribution function, modified to include mirror-trapped particles. The equation satisfied by  $g$  is

$$v_{\parallel} \mathbf{b} \cdot \nabla g + \mathcal{C}(g) = v_{\parallel} \mathbf{b} \cdot \nabla \phi \exp(-\varepsilon/T) \quad (2)$$

where  $\mathcal{C}$  is the collision operator linearized about a background Maxwellian of temperature  $T$ . [The adjoint technique used to derive Eq. (1) is essentially the same procedure as that used earlier in the mirror program [22] to relate the collisional loss rate of an electrostatically confined species in the presence of passing particles to the solution with no passing particles.] Note that some sign errors in Sec. II of Refs. [3] and [21] are corrected here. We bounce average Eq. (2), expanding  $g$  in increasing powers of the ratio of the collision frequency to the transit (or bounce) time. To leading order,  $g = 0$  for trapped particles, while for passing particles, the equation for  $g$  is

$$\left\langle \frac{B}{|v_{\parallel}|} \mathcal{C}(g) \right\rangle = \pm \left\langle \frac{\mathcal{R}_t}{R} \right\rangle \exp(-\varepsilon/T) \quad , \quad (3)$$

where the upper (lower) sign is for positive (negative)  $v_{\parallel}$  and  $\mathcal{R}_t = B_t/B_0$ .

We evaluate the bounce-averaged collision operator in the high-energy (but non-relativistic) limit  $mv^2/2T \gg 1$ . To leading order in  $T/mv^2$ , the equation is separable in the speed  $v$  and  $\eta = v_{\perp 0}^2/v^2$ , where the subscript 0 denotes evaluation at the field minimum (outside of the flux surface). Hence we can write  $g = [\langle \mathcal{R}_t/R \rangle c^4/(4\nu v_t^3)] \exp(-\varepsilon/T) F(v) H(\eta)$  where  $F(v) = (v/c)^4$ ,  $\nu = 4\pi n e^4 \ln \Lambda / m^2 v_t^3$ ,  $v_t = (2T/m)^{1/2}$  and  $\hat{Z} = (1 + Z)/2$ , with  $Z$  the charge state. Then we can reduce Eq. (3) to an ordinary differential equation for  $H(\eta)$ ,

$$- \left\langle \frac{\mathcal{R}v}{|v_{\parallel}|} \right\rangle H + \hat{Z} \frac{d}{d\eta} \eta \left\langle (1 - \mathcal{R}\eta)^{1/2} \right\rangle \frac{dH}{d\eta} = \pm 1 \quad . \quad (4)$$

Here,  $\mathcal{R} = B/B_0$  is the local mirror ratio on a field line. The boundary conditions to be satisfied are that  $H$  be regular at  $\eta = 0$  and vanish at the trapped-passing boundary  $\eta = \eta_s \equiv B_0/B_{\max}$ . ECRH current-drive efficiencies obtained from numerical solution to Eq. (4) were presented by Yoshioka and Antonsen [23].

We now make the square-well approximation: in mirror physics, it is often found that semi-quantitative properties of solutions to bounce-averaged Fokker-Planck problems can be obtained by replacing the bounce-averaged collision operator by the local operator evaluated at the bottom of the magnetic well. Making that approximation here, and introducing the variable  $\lambda = \pm(1 - \eta)^{1/2} = v_{\parallel}/v$ , Eq. (4) becomes an inhomogeneous Legendre equation,

$$-4H + \hat{Z} \frac{d}{d\lambda} (1 - \lambda^2) \frac{dH}{d\lambda} = 4\lambda \quad .$$

This equation can be solved analytically. The solution which satisfies the aforementioned boundary conditions is:

$$H = \frac{-4\lambda}{(Z + 5)} \left[ 1 - \frac{\lambda_s}{|\lambda|} \frac{P_{\alpha}(|\lambda|)}{P_{\alpha}(\lambda_s)} \right] \quad (5)$$

where  $P_\alpha$  is a Legendre function with index  $\alpha$  satisfying the relation

$$\alpha(\alpha + 1) = -4/\hat{Z} \quad . \quad (6)$$

and  $\lambda_s = (1 - \eta_s)^{1/2}$ . The solution given in Eq. (6) reduces the calculation of the current driven by any wave including trapped-particle effects to quadrature, assuming the wave-induced flux  $\Gamma_w$  is known (which, in particular, is true for weakly heated plasmas where the distribution function is nearly Maxwellian). The solution is easily generalized to be semi-relativistic as described in Ref. 3.

To see how well the square-well approximation holds up, we calculate a specific example, nonrelativistic ECRH current drive. For each intersection of a ray of ECRH with a flux surface, the current-drive efficiency given by dividing the current from Eq. (1) by the absorbed flux-surface-averaged power density reduces to:

$$\frac{J_0}{P_d} = \frac{-m^2 c^4 \int d\varepsilon \gamma [D_{\varepsilon\varepsilon} \mathcal{L}(f) \mathcal{L}(FH)]_{p_{\parallel a}, \theta_a}}{8T \int d\varepsilon \gamma [D_{\varepsilon\varepsilon} \mathcal{L}(f)]_{p_{\parallel a}, \theta_a}} \quad (7)$$

where  $D_{\varepsilon\varepsilon}$  is the ECRH energy diffusion coefficient,  $\mathcal{L} = \partial/\partial\varepsilon + (k_{\parallel}/\omega)\partial/\partial p_{\parallel}$ ,  $p_{\parallel a}$  is the resonant parallel momentum  $m(\gamma\omega - \ell\Omega)/k_{\parallel}$ ,  $\omega$  is the wave frequency,  $\Omega$  is the nonrelativistic cyclotron frequency,  $\ell$  is the harmonic number,  $k_{\parallel}$  is the parallel wave number, and  $\theta_a$  is the poloidal angle at which the ray intersects the flux surface. Here, the current density is given in units of  $env_t$  and the power in units of  $nmv_t^2\nu$ , and the current density is related to its value at the outside of the flux surface according to  $J/J_0 = B/B_0$ .

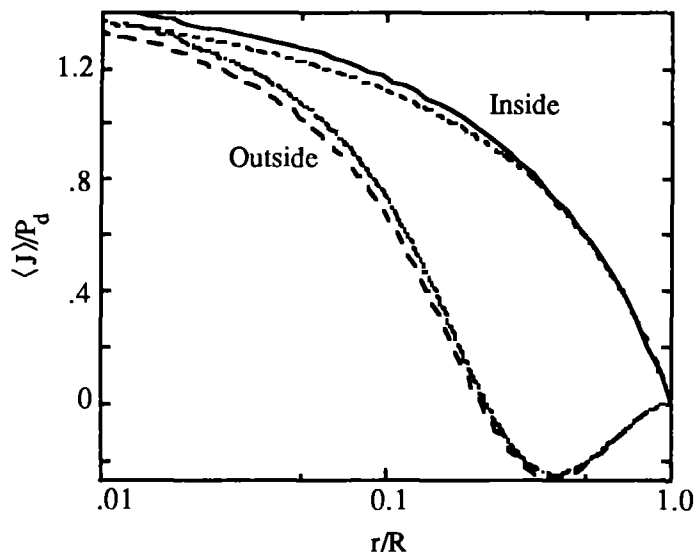


FIG. 1. Nonrelativistic ECRH current-drive efficiency vs. inverse aspect ratio for  $\varepsilon_0/T = 10$  and  $\Omega/\omega = 0.9$ . Solid and dotted curves are for  $H$  determined numerically from Eq. (4) for circular flux surfaces of radius  $r$ ; dashed curves are for the square-well model.



In Fig. 1, we compare results obtained from Eq. (7) using the Green's function determined numerically from Eq. (4) and the analytic square-well result Eq. (5). We plot the current-drive efficiency versus inverse aspect ratio for fundamental ECRH resonance on the inside and outside extremes of a flux surface for a Maxwellian electron distribution and  $\varepsilon_0/T = 2$ , where  $\varepsilon_0$  is the minimum resonant energy. It is apparent that the square-well approximation is quite good, agreeing to within a few percent except when the efficiency is near zero. This agreement holds over a broad range of parameters. Figure 1 also illustrates that current drive is more efficient for resonance on the inside of the flux surface than the outside; this is because ECRH heating on the inside does not move passing particles toward the trapped-passing separatrix. For resonance on the outside, we observe the current reversing at moderate-to-large inverse aspect ratio; this is the “Ohkawa effect” [24], whereby the reverse current associated with a wave-induced push of an initially passing electron into the trapped region dominates.

#### IV. ECRH-Driven Potentials

In thermal-barrier tandem mirrors, ECRH is usually applied at the thermal barrier to enhance the barrier potential. The mechanism is that the ECRH generates a population of energetic, mirror-confined electrons which do not respond appreciably to the potential variations (which are small compared to hot-electron energies); quasineutrality requires that thermal electrons be pushed away, which is effected by the potential becoming locally more negative. The effect is particularly strong on a transient basis if the ECRH is applied in a pulse short compared to ion transit time scales, since then the potential can form before ions can flow into the resulting potential well; this was observed in the Berkeley Multiple Mirror Experiment MMX [20]. The shortness of the time scale accomplishes the same thing as pumping of a steady-state thermal barrier, namely keeping the trapped-ion phase space relatively empty.

The same potential-generation mechanism is also operative when ECRH heating is applied to a finite-aspect-ratio tokamak, and should be particularly effective when the ECRH is applied in short pulses, as in the Microwave Tokamak Experiment (MTX) under construction at Livermore [25]. (MTX is the Alcator-C tokamak from MIT, heated by a free-electron laser driven by the ETA-II electron accelerator at Livermore.)

We calculate the potential on a time scale short compared to ion-transit times by dividing the electrons into a cold population with a Maxwell-Boltzmann distribution (and potential response), and a hot group which is assumed not to respond to the potential and is modelled as a bi-Maxwellian at the point along a field line where the ECRH is resonant:

$$f_h = C \exp[-(\varepsilon_\perp/T_\perp + \varepsilon_\parallel/T_\parallel)] \quad . \quad (8)$$

Here,  $\varepsilon_{\perp}$  and  $\varepsilon_{\parallel}$  are the perpendicular and parallel energies at the resonance point,  $T_{\perp}$  and  $T_{\parallel}$  are the perpendicular and parallel temperatures, and  $C$  is a normalization constant to be determined. The temperatures  $T_{\perp}$  and  $T_{\parallel}$  are prescribed in the present calculation, but in principle are determined by the dynamics of particle motion in the intense heating field and competition with collisions (see, it e.g., Sec. V). The ions are treated as a background of uniform density  $n_0$ . The calculation is described in more detail, and extended to longer time scales, in Ref. 20.

We assume that the hot electrons are collisionless on the transit time scale; the hot-electron distribution is then everywhere given by Eq. (8), as  $\varepsilon_{\perp}$  and  $\varepsilon_{\parallel}$  are constants of motion (related to local variables through constancy of energy and magnetic moment). Then the local hot-electron density is given by

$$\begin{aligned} n_h(s) &= \frac{4\pi\mathcal{R}(s)}{m^2} \int \frac{d\varepsilon_{\perp}d\varepsilon_{\parallel}}{v_{\parallel}} f_h \\ &= \left(\frac{2\pi T_{\parallel}}{m}\right)^{3/2} C\lambda g(\mathcal{R}) \end{aligned} \quad (9)$$

where  $\mathcal{R}(s) = B/B_r$  is the mirror ratio relative to the resonance position  $r$ ,  $\lambda \equiv T_{\perp}/T_{\parallel}$ , and

$$g(\mathcal{R}) = \begin{cases} \frac{\mathcal{R}}{1 + [\lambda(1 - \mathcal{R})]^{1/2}} & , \quad \mathcal{R} \leq 1 \\ \frac{\mathcal{R}}{1 + [\lambda(\mathcal{R} - 1)]} & , \quad \mathcal{R} \geq 1 \end{cases} .$$

We normalize the hot-electron distribution so that the total number of hot electrons on a flux tube is a fraction  $\eta$  times the total electron number; this determines  $C$  so that

$$n_h = \hat{\eta} n_0 g(r) \quad (10)$$

with  $\hat{\eta} = \eta / \langle g \rangle$  and  $\langle \rangle$  denotes a  $\int ds/B$  average along a field line.

One may verify from Eqs. (9) and (10) that the hot-electron density peaks at the resonance position (where  $g = 1$ ) and that, depending on values of  $\lambda$  and  $\mathcal{R}$ , the maximum relative variation in hot-electron density occurs for resonance at either the bottom or top of the magnetic well.

The potential variation is determined by quasineutrality,

$$\frac{\Phi - \Phi_*}{T_e} = \ln \frac{n_0 - n_h(s)}{n_0 - n_h(s_*)} = \ln \frac{1 - \hat{\eta}g(\mathcal{R})}{1 - \hat{\eta}g(\mathcal{R}_*)} \quad , \quad (11)$$

where  $s_*$  denotes some convenient reference point.

The calculated potential becomes singular at  $\mathcal{R} = 1$  when  $\hat{\eta} = 1$ . From (10) it follows that this always occurs for the hot-electron fraction  $\eta$  less than one, as

it can be seen from (9) that  $\langle g \rangle < 1$ . Thus, if the ECRH is on long enough, the heating process extinguishes itself (that is, the potential shuts off the flow of cold electrons into the heating zone) before all of the cold electrons are converted to hot. With a more realistic model in which the hot-electron response to the potential is retained, the potential would never become singular, but it would become of the order of the hot-electron energy, which would still be adequate to turn off the flow of cold electrons assuming  $\lambda$  is large. Additional fueling can occur only on the time scale of the ion motion.

For the particular case of a circular cross-section tokamak with  $B^{-1} \propto 1 + \delta \cos s/s_0$  with  $\delta = r/R$  and resonance at the inside of a flux surface, an explicit closed-form expression for  $\langle g \rangle$  is obtainable,

$$\langle g \rangle = \begin{cases} \frac{4}{\pi} \frac{\arctan \xi}{(1 - K^2)^{1/2}} & , \quad K < 1 \\ \frac{2}{\pi} \frac{\ln \frac{1+\xi}{1-\xi}}{(K^2 - 1)^{1/2}} & , \quad K > 1 \end{cases} \quad (12)$$

where  $\xi = |(K-1)/(K+1)|^{1/2}$  and  $K = (2\lambda\delta)^{1/2}$ . Top-of-well heating is of interest for tokamaks because it minimizes trapped-particle effects on current drive (see Sec. III) and, as will be discussed below, it minimizes toroidal variations of the ECRH-driven potential.

We consider application of the results to operation of MTX with a density of  $10^{14} \text{ cm}^{-3}$  and a range of background electron temperatures  $T_e$ . The expected microwave field is sufficient to raise the perpendicular energy of a 1 keV electron to as much as 10 keV on a single pass through resonance. We evaluate the hot-electron anisotropy parameter  $\lambda \equiv T_{\perp}/T_{\parallel}$  by taking  $T_{\parallel} = T_e$  and  $T_{\perp}$  to be half the maximum amplitude of the energy oscillations of electrons in the intense microwave field [25,26]. From Refs. 25 and 26, this implies, for fundamental ordinary mode heating in MTX,  $\lambda \approx 5T_e^{-2/3}$  with  $T_e$  in keV. The pulse duration  $\tau_p$  limits the hot-electron fraction to about the ratio of  $\tau_p$  to the mean electron toroidal transit time, giving  $\eta \approx 0.25T_e^{1/2}$  on a heated flux surface. For heating on the inside of the flux surface at  $\delta = r/R = 0.1$ , we obtain from Eqs. (10)-(12) the results shown as the curve labelled “e” in Fig. 2.

We note that the expected range of electron temperatures is about 1–2.5 keV [25]. Over this range,  $\Delta\Phi/T_e \approx 0.3 - 0.5$ . Results at lower  $T_e$  are relevant to startup. Note that  $\Delta\Phi/T_e$  increases with increased  $T_e$ ; this is because the increase in the hot-electron fraction (due to the increased number of electrons passing through the microwave beam during the time  $\tau_p$ ) more than compensates for the decreased anisotropy. The divergence of the potential at  $T_e$  of about 10 keV is the singularity associated with the choking off of the flow of background (“cold”)

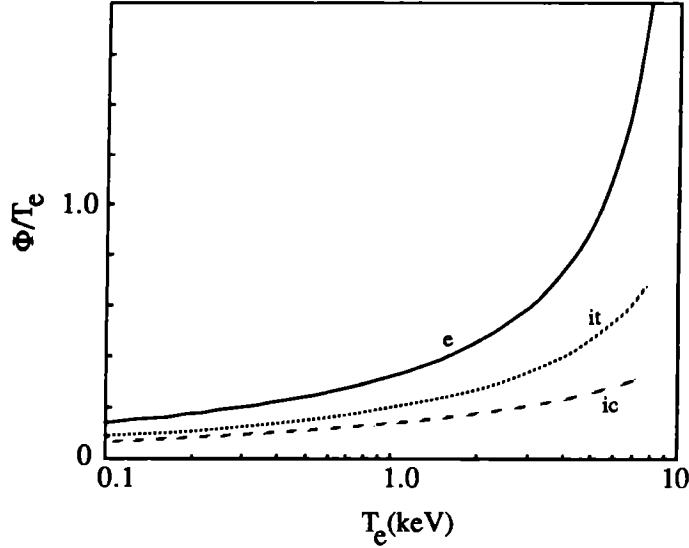


FIG. 2. Expected buildup of potential variation along a field line  $\Delta\Phi$  versus cold electron temperature  $T_e$  for the MTX experiment, on the (e) hot-electron transit time scale, (it) ion transit time scale and (ic) ion collisional time scale.

electrons discussed earlier; however, the neglect of the hot-electron response to the potential invalidates the curve beyond  $T_e \approx 4$  keV. Also shown in Fig. 2 are the potentials on the ion-transit and ion-collision time scales, obtained from Ref. 20. (The latter result is essentially an academic exercise for MTX, as the hot electrons relax on a time scale similar to the ion collision time.)

The potential structures are fundamentally variations along field lines. However, since the heating is typically localized in directions transverse to field lines, one can expect potential variations in those directions as well. Of particular interest are axisymmetry-breaking potential variations (toroidal in a tokamak, azimuthal in a mirror), as such variations are likely to significantly enhance neoclassical transport. Consider a tokamak with a toroidally localized microwave source. To the extent that the hot electrons are all passing (most nearly true for heating resonant on the inside of the flux surface) then on an irrational flux surface, the hot electrons flow over the entire surface, producing only a poloidal density and hence potential variation. Trapped hot electrons, however, fill the flux surface only on the relatively slow drift time scale. When this time scale is comparable to or longer than hot-electron and ion collision times (as in MTX), the potential must vary toroidally as well as poloidally. Since production of trapped hot electrons is minimized for resonance on the inside of a flux surface (see Sec. III), this choice minimizes toroidal potential variation for heating on irrational flux surfaces. On a rational surface, a field line does not cover the flux surface; hence, in the neighborhood of a rational surface, potential variation is confined approximately to a helical band of field lines which pass through the microwave beam.

Other possible consequences of these time-dependent, ECRH-generated potentials include parametric coupling to low-frequency modes of the plasma, modification of current-drive efficiency, and enhanced ion heating. The latter arises because, on the ion-transit time scale, ions flowing into the potential wells set up by the hot electrons are accelerated, and then tend to equilibrate with the background ions trapped in the well on an ion-ion scattering time scale (faster than the hot-electron-ion time scale in which the ions would otherwise be heated by the hot electrons). If the potential variation is large compared to the background ion temperature, a faster relaxation due to a two-stream instability is possible.

## V. Strongly Heated Distribution Functions\*

In order to be effective in enhancing the thermal-barrier potential dip, the ECRH applied in a tandem mirror must be strong enough to render the electron distribution appreciably non-Maxwellian. For tokamak heating and current-drive applications, distortion of the distribution from Maxwellian is not required, but typically does occur at power levels required to drive appreciable current. Furthermore, the theory presented in Sec. III indicates that such distortion can be helpful in raising the current-drive efficiency (see, *e.g.*, Ref. 3), while the calculation in Sec. IV demonstrates that the distortion can generate significant potential variations. Thus calculations of strongly-heated distribution functions, which are of central importance for tandem mirrors, are also of appreciable interest for tokamaks; significant contributions have been made by theorists from both communities (see, *e.g.*, Refs. 27 and 28). The discussion which follows deals explicitly with electron-cyclotron heating, but the general framework is applicable to other heating schemes (such as lower hybrid) as well.

The calculations required for tandem mirrors and tokamaks have a similarity which arises, oddly enough, out of the disparity in scale lengths for the two devices. In general, at a particular point along a field line, the resonance condition for a cyclotron wave,  $\gamma\omega - \ell\Omega - k_{\parallel}p_{\parallel}/m = 0$ , corresponds to a single (curved) line in either local momentum space or in energy-magnetic moment ( $\varepsilon$ - $\mu$ ) space. This curve shifts as the magnetic field changes along a field line. In a tandem mirror, because mirror ratios are large, the scale length for appreciable change in the resonance curve is comparable with or shorter than a typical scale length for the wave illumination profile. Consequently, large portions of  $\varepsilon$ - $\mu$  space correspond to particles which resonate with the wave somewhere within the wave illumination profile. But because of the multi-cell nature of the device,  $\varepsilon$ - $\mu$  space is divided into regions in which the relative roles of wave heating and collisions may be quite different. In a tokamak, there is, usually, only one well, but the small mirror ratio

---

\*The calculations in this section were done in collaboration with I. B. Bernstein and V. Chan

present within the wave illumination profile implies that the range of resonance curves can be significantly limited. The net result is that, for either device,  $\varepsilon$ - $\mu$  space can be divided into regions where waves dominate and where collisions dominate; the theoretical task is to solve the appropriately ordered kinetic equations in each region, with suitable boundary conditions providing the link between regions. An example of this calculation for tandem mirrors is given in Ref. 27 and is the subject for my workshop presentation at this School. Here, we describe such a calculation for tokamaks.

It is convenient to use as variables the energy  $\varepsilon$  and  $x = \varepsilon - \mu mc\omega/\ell$ . The level curves  $x = \text{const.}$  are the heating characteristics [29] along which the cyclotron wave moves particles. The characteristics and the resonance band are sketched for the case  $N_{\parallel} \equiv k_{\parallel}c/\omega < 1$  and  $Y \equiv \ell\Omega/\omega < 1$  in Fig. 3.

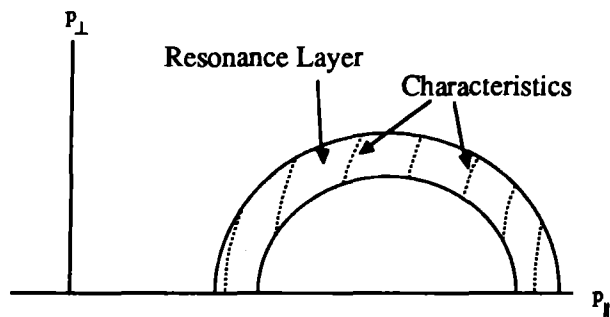


FIG. 3. Sketch of characteristics (dashed curves) and resonance band (bounded by solid curves) for cyclotron heating with  $N_{\parallel} < 1$  and  $Y < 1$ .

The kinetic equation has the form:

$$\frac{\partial}{\partial \varepsilon} D \frac{\partial f}{\partial \varepsilon} + \mathcal{C}(f) = 0 \quad (13)$$

where  $\mathcal{C}$  is the transit time times the collision operator, and the r.f. diffusion coefficient  $D$  is zero outside the resonance band. We seek the form of the distribution function inside the resonance band, as that is sufficient to determine the current-drive efficiency [3].

We assume that the resonant region is in the high-velocity tail of the distribution function, so that the collision operator can be approximated by the linearized operator corresponding to scattering of test particles off of a Maxwellian background. Then  $\mathcal{C}$  has the properties that it is a second-order partial differential operator in the variables  $\varepsilon, x$ , and, in particular, has the form of a divergence of a flux in these coordinates,  $\mathcal{C}(f) = -\partial_x \Gamma_{cx} - \partial_\varepsilon \Gamma_{c\varepsilon}$ .

We now proceed to the strong r.f. limit, in which the r.f. operator dominates over collisions inside the resonance band. We treat this as previously described for

tandem mirrors [30]. From the form of the expressions derived below, it can be seen that the diffusion coefficient required for validity of the procedure increases with the width of the resonance layer. For a broad layer, one can back away from this essentially infinite r.f. limit by doing an explicitly two-dimensional calculation in the layer, of the sort described in Ref. 27 and in my workshop presentation.

To leading order in an expansion in inverse powers of  $D$ ,  $f$  is constant on characteristics,  $f_0 = f_0(\varepsilon)$ . Integrating the next-order equation in  $\varepsilon$  across the resonance band yields a consistency relationship which relates a second-order ordinary differential operator (in  $x$ ) operating on  $f_0$  to the first-order r.f.-driven flux across the boundaries of the resonance band:

$$\hat{C}(f_0) = \Gamma_{r\varepsilon} \Big|_{\varepsilon_1}^{\varepsilon_2} \quad (14)$$

where  $\hat{C} \equiv \int d\varepsilon \mathcal{C}$  is the aforementioned ordinary differential operator,  $\varepsilon_1$  and  $\varepsilon_2$  are the boundaries of the resonance band (functions of  $x$ ), and  $\Gamma_{r\varepsilon} = -D\partial_\varepsilon f_1$ . Integrating Eq. (13) across a resonance-band boundary yields a flux-conservation condition which can be used to eliminate  $f_1$ ,

$$\Gamma_{r\varepsilon} = \frac{d\varepsilon_j}{dx} \Gamma_{cx}(f_0) + \Gamma_{cn} \quad (15)$$

where  $\Gamma_{cn} = \Gamma_{c\varepsilon} - (d\varepsilon_j/dx)\Gamma_{cx}$  evaluated just outside the resonance layer, and  $j = 1, 2$ . The problem is closed, *i.e.* Eq. (14) becomes a one-dimensional equation for  $f_0$ , if we can derive a relationship between the collisional flux  $\Gamma_{cn}$  and  $f$  along the boundaries.

We can derive such a relationship from the Green's function for the collision operator in an unbounded domain (all physical  $\varepsilon, x$ ). The technique is similar to that used for tandem mirrors in Ref. 22. Let the Green's function  $G(x, \varepsilon, x_0, \varepsilon_0)$  satisfy

$$-\mathcal{C}(G) \equiv \nabla \cdot \Gamma_c(G) = \delta(x - x_0)\delta(\varepsilon - \varepsilon_0) \quad (16)$$

where the  $\nabla$  operator is evaluated in  $\varepsilon, x$  coordinates as if they were rectangular. In the nonrelativistic limit,  $G$  can be written explicitly in terms of Legendre polynomials and Kummer functions. The Fokker-Planck equation for the actual distribution function  $f$  outside the resonant layer is

$$\nabla \cdot \Gamma(f) = 0 \quad (17)$$

coupled with the boundary conditions that  $f$  and the flux be continuous at the boundary with the resonant layer. Now we note that  $\Gamma(f)$  has the form:  $\Gamma = -\vec{C} \cdot \nabla(f/f_M)$  where  $f_M = \exp(-\varepsilon/T)$  is proportional to a Maxwellian distribution function, and  $\vec{C}$  is a symmetric tensor. Multiplying Eq. (16) by  $f/f_M$  and Eq. (17)

by  $G/f_M$ , subtracting, integrating the resultant equation over a collisional domain (one of the two domains outside the resonance layer), and taking  $x_0, \varepsilon_0$  to be within the domain, we obtain

$$\int \frac{ds}{f_M} \mathbf{n} \cdot (f\Gamma(G) - G\Gamma(f)) = \frac{f(x_0, \varepsilon_0)}{f_M(\varepsilon_0)}$$

where  $ds$  is an increment along the boundary in  $x, \varepsilon$  space and  $\mathbf{n}$  is a unit outward (into the r.f. region) normal. Letting  $x_0, \varepsilon_0$  approach a boundary and writing the integral explicitly as an integral over  $x$ , we have an integral equation relating  $f$  and the flux  $\Gamma_{cn}$  which appears in Eq. (14),

$$\int \frac{dx'}{f_M} (K(x, x')f - G(x, x')\Gamma_{cn}) = -\frac{f(x, \varepsilon_j(x))}{f_M} \quad (18)$$

with

$$K(x, x') \equiv \Gamma_{ce} [G(x, \varepsilon_j(x), x', \varepsilon_j(x'))] - \frac{d\varepsilon_j}{dx} \Gamma_{cx}(G) \quad .$$

There are two such equations, with  $j = 1, 2$ .

Using Eqs. (14) and (15) we can eliminate, say,  $\Gamma_{cn}(\varepsilon_2)$  in favor of  $\Gamma_{cn}(\varepsilon_1)$  and  $f_0$  in Eqs. (18). Eqs. (18) then constitute a set of two coupled one-dimensional integral and integro-differential equations for the remaining pair of variables. Integration by parts can be used to convert the integro-differential equation into an integral equation.

The net result of the calculation is thus the conversion of a two-dimensional partial differential equation into two coupled one-dimensional integral equations, which can be solved much faster. We are presently exploring the possibilities for approximate analytic solutions.

## VI. Survey of Other Areas

In this section we discuss other areas of toroidal physics where a mirror-theoretic point of view has been or should be helpful.

Bean-shaped tokamaks have some noteworthy similarities to tandem mirrors. Moving along a field line in a bean tokamak, one finds, as in a tandem mirror, a relatively short, small-mirror-ratio, good-curvature magnetic well and a relatively long, larger-mirror-ratio well with unfavorable curvature. It has been suggested [31] that one might enhance stability in a bean tokamak by providing extra pressure weighting to the good curvature well; this could be arranged by driving an electron or ion anisotropy through cyclotron-resonance heating in the good well. As in the discussion of Sec. IV, the anisotropy will be accompanied by a potential difference between the good and bad curvature cells, adding to the analogy with tandem mirrors. To study the scheme, one would want to do multi-region Fokker-Planck



calculations and MHD calculations with anisotropic pressures — both areas in which computational tools and analytic expertise have been developed for mirror systems.

An area where mirror physics is clearly applicable is in the edge region of a toroidal device, where field lines ultimately intersect material structures (walls, limiters or divertors). For a tokamak which is hot just inside the separatrix dividing closed and open field lines (so that collision times are longer than banana periods), the mirror-like region extends a banana width into the closed-field-line region. Ohkawa has pointed out [9,32] that the total energy confinement time can be determined by the confinement time in this mirror region, underscoring the importance of understanding this region. Some interesting work has been done. Hinton [10], for example, has developed a model for the H mode in a collisional edge region based on modelling endloss as a heat sink in classical transport equations. H-mode-like behavior (large temperature gradient at edge) can occur for a suitable orientation of the divertor x-point and a sufficiently large heat throughput. He and Ohkawa [32] have also noted that a hot, collisionless edge region also has an H-mode-like large temperature gradient, with a scale length of order of the ion banana width. More recently, Hinton has begun considering potential effects on these processes [33]. Again, the physics closely parallels that in a tandem mirror (see, e.g., Ref. 34.) On a given field line, electrons and ions are lost axially at different rates, setting up an ambipolar potential  $\Phi$ ; the variation of  $\Phi$  across field lines affects radial transport. The potential is determined by requiring equality of the net (radial and axial) electron and ion loss rates. For the case of the hot edge plasma, the presence of loss-cone distributions should present microstability issues similar to those studied for mirror plasmas.

Well into the interior of a toroidal plasma, mirror-like phenomena can arise if there are phase-space regions in which select groups of particles can be rapidly lost from the machine. This can occur for particles trapped in a toroidal ripple of a tokamak, for high-energy particles (alpha particles, for example) trapped in the main toroidal well of a tokamak, and for helically trapped particles in a stellerator, and has been suggested as a major loss mechanism for hot electrons in EBT-S [13]. If these losses are faster than the collisional replenishment rate, they, like endloss in a mirror, produce loss regions in velocity space where the distribution function to first approximation vanishes. The calculation of the distribution functions and the associated linear and quasilinear microstability analyses are analogues of mirror calculations. An example was provided by the concern [11] that trapped alphas might be rapidly lost from a tokamak reactor. While more recent work has indicated that the trapped alphas are probably confined [35], the ensuing analysis by Nevins [36] is of interest for its parallel to a mirror calculation. The distribution function is calculated by a Legendre-function expansion, as in the mirror-machine

case, only it is the passing region rather than the trapped region that is populated. If trapped alphas of sufficiently low energy were lost, the resulting distribution, projected onto the  $v_{\parallel}$  axis, would be nonmonotonic, implying an “anti-loss-cone”-driven mode analogous to the mirror alpha loss-cone instability [37]. For less severe conditions, the most likely candidate for instability is an anisotropy-driven mode, an analog of the anomalous Doppler instability.

## VII. Conclusion

We have discussed several areas in the physics of toroidal fusion devices where ideas from mirror theory have been or are likely to prove helpful. Our examples included the use of the square-well approximation to calculate trapped-particle effects on r.f. current drive, the calculation of r.f.-driven potentials, and the determination of distribution functions strongly heated by r.f., and we identified bean-shaped tokamaks, the edge regions of toroidal plasmas, and other regions where bad drifts cause direct particle losses as fertile hunting grounds for mirror theorists. Our purpose is not to provide an exhaustive survey or an in-depth account of work done, but only to illustrate by example that, in a fusion effort increasingly dominated by toroidal devices, mirror theory and mirror physics in general has a vital role to play.

## Acknowledgement

The author thanks W. M. Nevins and L. D. Pearlstein for helpful discussions and G. R. Smith for a careful reading of the manuscript. This work was performed under the auspices of the U.S. Department of Energy by the Lawrence Livermore National Laboratory under contract number W-7405-ENG-48.

## REFERENCES

- [1] MATSUDA, Y., STEWART, J. J., J. Comp. Phys. **66** (1986) 197.
- [2] McCOY, M. G., KERBEL, G. D., FRANZ, M., Bull. Am. Phys. Soc. **31** (1986) 1523.
- [3] COHEN, R. H., Phys. Fluids **30** (1987) 2442.
- [4] PASTUKHOV, V. P., Nucl. Fusion **14** (1974) 3.
- [5] CHERNIN, D. P., ROSENBLUTH, M. N., Nucl. Fusion **18** (1978) 47.
- [6] COHEN, R. H., RENSINK, M. E., CUTLER, T. A., MIRIN, A. A., Nucl. Fusion **18** (1978) 1229.
- [7] NAJMABADI, F., CONN, R. W., COHEN, R. H., Nucl. Fusion **24** (1984) 75.
- [8] CATTO, P. J. LI, X. Z., Phys. Fluids **28** (1985) 352.
- [9] OHKAWA, T., CHU, M. S., HINTON, F. L., LIU, C. S., LEE, Y. C., Phys. Rev. Lett. **51** (1983) 2101.
- [10] HINTON, F. L., Nucl. Fusion **25** (1985) 1457.
- [11] WHITE, R., Sherwood Theory Meeting, San Diego, April 1987.
- [12] STRINGER, T. E., Nucl. Fusion **12** (1972) 689.
- [13] BERRY, L. A., BAITY, F. W., BATCHELOR, D. B., BIENIOSEK, F. M., BIGELOW, T. S., COBBLE, J. A., COLCHIN, R. J., DAVIS, W. A., GLOWIENKA, J. C., GOYER, J.

- R., HASTE, G. R., HILLIS, D. L., HIROE, S., KIMREY, H. D., OWEN, L. W., OWENS, T. L., RICHARDS, R. K., SOLENSTEN, L., SWAIN, D. W., UCKAN, N. A., UCKAN, T., WILGEN, J. B., Proc. Internat. Conf., *Plasma Physics and Controlled Nuclear Fusion Research*, London, November 1984, IAEA-CN-44/Vienna, Vol. 2 (1985) 545.
- [14] BERK, H. L., FOWLER, T. K., PEARLSTEIN, L. D., POST, R. F., HORTON, W. C., ROSENBLUTH, M. N., Proc. Internat. Conf., *Plasma Physics and Controlled Nuclear Fusion Research*, Novosibirsk, August, 1968, IAEA-CN-24/Vienna, Vol. II (1969) 151.
  - [15] PEARLSTEIN, L. D., in *Physics Basis for an Axisymmetric Design for the End Plugs of MFTF-B*, D. E. Baldwin and B. G. Logan, editors, Lawrence Livermore Laboratory Report UCID-19359 (1982) 181.
  - [16] HOOPER, E. B. JR., COHEN, R. H., CORRELL, D. L., GILMORE, J. M., GRUBB, D. P., Phys. Fluids **28** (1985) 3609.
  - [17] MYRA, J. R., CATTO, P. J., FRANCIS, G. L., Phys. Fluids **29** (1986) 794.
  - [18] CHANG, C. S., HARVEY, R. W., Nucl. Fusion **23** (1983) 935.
  - [19] HSU, J. Y., CHAN, V. S., HARVEY, R. W., PRATER, R., WONG, S. K., Phys. Rev. Lett. **53** (1984) 564.
  - [20] LICHTENBERG, A. J., LIEBERMAN, M. A., COHEN, R. H., to be published in Phys. Fluids.
  - [21] ANTONSEN, T. M., HUI, B., IEEE Trans. Plasma Sci **PS-12** (1984) 118; ANTONSEN, T. M., CHU, K. R., Phys. Fluids **25** (1982) 1295.
  - [22] COHEN, R. H., BERNSTEIN, I. B., DORNING, J. J., ROWLANDS, G., Nucl. Fusion **20** (1980) 1421.
  - [23] YOSHIOKA, H., ANTONSEN, T. M., Nucl. Fusion **26** (1986) 839.
  - [24] OHKAWA, T., *Steady State Operation of Tokamaks by RF Heating*, General Atomic Report GA-A13847 (1976).
  - [25] THOMASSEN, K. I., Ed., *Free Electron Laser Experiments in ALCATOR C*, LLL-PROP-00202, Lawrence Livermore National Laboratory (U. S. Government Printing Office 1986-8-687-002/44101), July 1986.
  - [26] NEVINS, W. M., ROGNLIEN, T. D., COHEN, B. I., Phys. Rev. Lett. **59** (1987) 60.
  - [27] NEVINS, W. M., BOGHOSIAN, B. M., COHEN, R. H., CUMMINS, W. F., DUBOIS, P. F., FRIEDMAN, A., LODESTRO, L. L., MATSUDA, Y., PHILLIPS, M. W., PORTER, G. D., RENSINK, M. E., ROGNLIEN, T. D., PEARLSTEIN, L. D., SMITH, G. R., STEWART, J. J., Proc. Internat. Conf., *Plasma Physics and Controlled Nuclear Fusion Research*, Kyoto, November 1986, IAEA-CN-47/Vienna, paper C-II-1.
  - [28] FISCH, N. J. AND KARNEY, F. F., Phys. Fluids **28** (1985) 3107.
  - [29] ROGNLIEN, T. D., Phys. Fluids **26** (1983) 1545
  - [30] COHEN, R. H., Phys. Fluids **26** (1983) 2774
  - [31] PERKINS, F. W., Private Communication
  - [32] OHKAWA, T., *Combined Confinement System Applied to Tokamaks*, GA Technologies Report GA-A18393, May 1986, Submitted to Kakuyugo Kenkyu.
  - [33] HINTON, F. L., Sherwood Theory Meeting, San Diego, April 1987.
  - [34] MIRIN, A. A., AUERBACH, S. P., COHEN, R. H., GILMORE, J. M., PEARLSTEIN, L. D., RENSINK, M. E., Nucl. Fusion **23** (1983) 703.
  - [35] WHITE, R., Private Communication
  - [36] NEVINS, W. M., *An Alpha-Particle Analogue of the Anomalous Doppler Instability may be Important for Tokamak Alpha-Particle Distributions*, Lawrence Livermore National Laboratory MFE Theory Memorandum PT704002, April 16, 1987.
  - [37] HO, S. K., *An Alpha Loss-Cone Instability in the Central Cell of a Tandem Mirror Reactor*, Ph.D. thesis, University of Illinois, Urbana, Illinois USA (1987); HO, S. K., NEVINS, W. M., SMITH, G. R., MILEY, G. H., in preparation.

